1

Iterative Equalization of STSK-Aided Single-Carrier Systems: Design and Analysis with Non-Ideal Power Amplifiers

Talha Faizur Rahman, Vuk Marojevic, Senior Member, IEEE, and Claudio Sacchi, Senior Member, IEEE

Abstract—A plethora of new applications will be enabled by next generation wireless networks. These demand sophisticated medium access control and physical layer protocols in order to fulfill the requirements in terms of spectral efficiency, bit error rate (BER), energy efficiency, reliability, and security, among others. This paper develops an advanced space-time multiple-input, multiple-output (MIMO) solution that builds on the concept of space-time shift keying (STSK) for singlecarrier frequency domain equalization (SC-FDE). STSK-aided SC-FDE, or SSF, ensures space-time and frequency diversity in dispersive channels, but can only support suboptimal linear receiver schemes. We therefore introduce a turbo equalizer for SSF in frequency-selective multipath channels. It enables intersymbol-interference cancellation by means of iterative spacetime processing. We coin it the iterative space-time block equalizer (SSF-ISTBE). We provide the mathematical formulation for the proposed SSF-ISTBE framework in non-linear channel conditions. We demonstrate that the SSF-ISTBE achieves a substantial 4 dB gain in terms of BER over the linear minimum mean square error equalizer while significantly reducing the computational complexity of the optimal maximum likelihood SSF. When considering practical transceivers, in particular nonlinear power amplifiers, the gain of the SSF-ISTBE becomes more prominent over state-of-the-art approaches, demonstrating its robustness against non-linear distortion.

Index Terms—Single-carrier, MIMO, STSK, Iterative spacetime block equalizer, Frequency-domain equalization.

I. INTRODUCTION

Commercial wireless applications demand continuous advances of wireless communication systems to efficiently use the spectral resources and counter different types of impairments. The conceived applications of 5G and beyond are categorized as enhanced mobile broadband (eMBB), massive machine type communication (mMTC) and ultra-reliable low latency communication (URLLC) [1]. Compared to 5G, 6G systems will be needed to satisfy the increasingly heterogeneous communications requirements and to enable new applications and services. 6G networks are thus expected to offer [2]:

- ultra-high data rates of up to 1 Tbit/s;
- ultra-high energy efficiency;
- · massive low-latency access and response; and

Talha F. Rahman and Vuk Marojevic are with the Dept. of Electrical and Computer Engineering (ECE) at Mississippi State University, Mississippi State (MS) (email: tfr42@msstate.edu, email: vuk.marojevic@msstate.edu). Claudio Sacchi is with the University of Trento, Department of Information Engineering and Computer Science (DISI), 38123, Trento (Italy) and with the Consorzio Nazionale Interuniversitario per le Telecomunicazioni (CNIT), 43124, Parma (Italy) (email: claudio.sacchi@unitn.it)

 extended frequency band operation, from microwave to visible light communications.

It is expected that mobile channels are going to severely limit the performance of wireless systems in achieving the aforementioned goals.

Mobile wireless channels are characterized as frequency selective inducing severe inter-symbol interference (ISI). In this regard, orthogonal frequency division multiplexing (OFDM) and cyclic-prefix single-carrier transmission with frequency domain equalization, hereafter SC-FDE, are proven to be effective against ISI [3]. The applications of the aforementioned physical layer (PHY) techniques depend on the offered features. OFDM enables simpler receiver implementation while suffering from high peak-to-average power ratio (PAPR). Thanks to its increased diversity, SC-FDE signaling with the addition of cyclic prefix (CP) is more robust against frequency-selective multipath channels with sub-optimal low-complex receivers, while maintaining low PAPR. For this reason, SC-FDE is being considered as a potential candidate for future wireless systems.

Recently, researchers have started investigating SC-FDE for its resilience against Doppler effects, making it a favorable choice for vehicular applications [4]. On the other hand, the Doppler spread has detrimental effects on OFDM, destroying orthogonality of subcarriers and causing irreducible error floors. This compels the need for complex algorithms at the receiver to overcome the performance degradation, hence increasing the overall computational complexity of the system. Both OFDM and SC-FDE provide multiple-input, multipleoutput (MIMO) extensions, and different variants of MIMO are supported by the aforementioned transceivers. These include spatial modulation [5], spatial multiplexing [6] and space-time block coding [7], to name a few, and are considered for systems with different application requirements in terms of bit error rate (BER), data rate, energy and spectral efficiency, or other criteria. A multi-purpose MIMO scheme providing numerous advantages over the aforementioned techniques by combining space-time block coding with index modulation (IM) is proposed in [8] and is known as space-time shift keying (STSK). STSK-systems enable a flexible trade-off between diversity and multiplexing in dispersive environments.

Because of its characteristics, STSK is being considered as the potential MIMO candidate for applications that are demanding high data rates with stringent error rate requirements, see [9]. Of particular interest is the STSK-aided SC-FDE system, or SSF, which is well-suited for mobile wireless

applications. One of the biggest hurdles in achieving near optimum performance is the lack of efficient receiver designs. To this aim, we propose a novel frequency domain turbo equalizer that operates iteratively to minimize the residual ISI in space-time blocks at the output of the demodulation process. We coin it iterative space-time block equalization for SSF (SSF-ISTBE). The SSF-ISTBE is able to minimize the residual ISI in highly dispersive channels and, as a result, to increase the signal-to-interference plus noise ratio (SINR). This paper provides the following contributions:

- The ISTBE is proposed for SSF MIMO systems leveraging IM.
- We analytically derive the parameters for near-optimal performance of the proposed ISTBE receiver.
- We provide analytical closed-form expressions for feedforward and feedback coefficients in the presence of nonlinear solid state power amplifiers (SSPAs). The nonlinear SSPA is modeled using the simple, yet accurate Bussgang's theorem which allows evaluating the impact of non-linear distortion on the proposed framework.
- The detailed computational complexity analysis shows the trade-offs between performance and complexity.

The paper is structured as follows: Section II discusses the related work. In section III we define the system model. Section IV introduces the SSF-ISTBE and models the impact of non-linear HPAs as part of the proposed framework. Section V provides details about the simulation setup, and analyzes the performance and complexities. Finally, the conclusions are drawn in Section VI.

<u>Notations:</u> Throughout the paper we use the following notations: bold typefaces denote block of symbols and matrices, whereas, regular typefaces denote single symbol and its corresponding matrices; $(\cdot)^*$ and $(\cdot)^H$ denote the complex conjugate and Hermitian operations, respectively; $vec(\cdot)$ represents the vectorial stacking operation; \mathbb{I}_N denotes the identity matrix of the size $N \times N$. The expectation operation is denoted as $E(\cdot)$.

II. RELATED WORK

STSK-based systems, such as STSK-OFDM [8], have shown remarkable performance in narrowband channels where individual carriers are experiencing flat flading. However, their performance is significantly impacted by frequency selective wideband channels. This is witnessed in [10] where STSK-aided single carrier-FDMA (SC-FDMA) are proposed for dispersive channels. STSK-aided SC-FDMA, due to the inherent multipath frequency diversity, shows performance improvements over STSK-OFDM systems with sub-optimal linear receivers (MMSE and ZF). However, the performance of general MIMO-OFDM systems with a sub-optimal MMSE receiver erodes in dispersive fading channels. Also, the STSK-OFDM performance is severely limited in practice due to its high PAPR [11]. In [11], STSK-aided constant envelope OFDM is proposed for future wireless systems because it completely overcomes the SSPA non-linearity by exhibiting 0 dB PAPR at the cost of reduced spectral efficiency [12]. For this reason, SC-FDE with cyclic prefix has been widely considered for single-carrier systems in dispersive environments. SC-FDE is robust against frequency selective channels [3] and against non-linear SSPAs due to its reduced envelope fluctuations without sacrificing the spectral efficiency.

The authors of [13] justify the superiority of the MIMO-SC waveform over its OFDM counterpart in millimeter wave channels and, moreover, analyze the robustness of the former against hardware impairments. The inherent residual interference in MIMO-enabled SC-FDE systems severely reduces the diversity order in time-dispersive channels when sub-optimal linear equalization is employed. Since linear receivers are not capable of removing the interference we need to study non-linear iterative approaches for MIMO-enabled SC-FDE. A non-linear equalizer based on the turbo principle, as first proposed in [14], is considered for massive MIMO SC-FDE in [15] where the proposed approach shows performance close to that of a matched filter bank (MF). Similarly, SC spatial modulation (SC-SM) systems with the turbo receiver in the time domain is proposed in [16]. A frequency domain version of the turbo equalizer for SC-SM system is considered in [17] and enables soft-decision feedback for canceling the residual interference. Similarly, [18] proposes the a-priori informationbased iterative turbo equalizer for SC-SM in dispersive channels. A turbo equalizer with generalized approximate message passing is considered for SC-SM systems in [19]. Another variant of the turbo equalizer is proposed in [20] for generalized SC-SM systems and enables performance improvements by adopting unique feedback information for the demodulation process. From the aforementioned works it is evident that different flavors of the turbo equalizer can be conceived for performance improvement.

To the best of our knowledge, non-linear block equalization in the framework of SSF-ISTBE have not been studied. Moreover, none of the aforementioned works deals with non-linear distortions incorporated in the DFE framework. The authors of [21] use the linear approach proposed in [10] for STSK-aided SC-FDE systems in millimeter wave channels. The STSKaided SC-FDE with a linear MMSE receiver outperforms spatial modulation (SM)-aided SC-FDE in the presence of hardware impairments and channel estimation errors. However, a comparative analysis between SC-FDE and OFDM considering optimal and sub-optimal receiver architectures has not been analyzed in open literature. Moreover, the SSPA of RF front-ends considerably contributes to the cost and size of the transmitter. Therefore, SC transmission for IoT applications is studied in [22] because it provides path diversity gain, low transmission complexity, and low PAPR.

We, therefore, present a cost-effective and efficient solution that can be regarded as an important step-ahead of [21]. Specifically, we introduce a frequency domain turbo equalization based on an iterative approach to cancel the residual interference in frequency selective channels in the presence of non-linear distortions. Such an approach provides near-optimal performance for the considered SSF-framework when compared against state-of-the-art approaches. The proposed transceiver is particularly suitable for the uplink, which may use inexpensive SSPA in the transmitter.

Our framework is well-suited for various applications and the 6G service type eMBB + URLLC, which demands not just low error rates but also low latency. It is worth mentioning

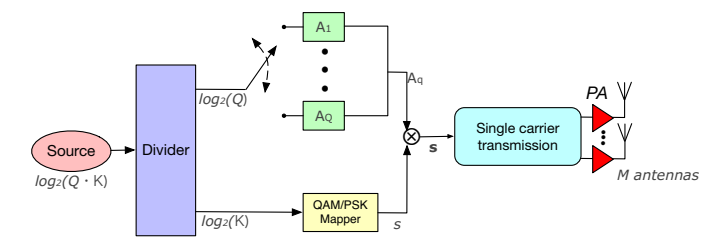


Fig. 1. Transmitter architecture of the SSF system with PA.

that in 6G systems there will be application-specific physical layer designs. The proposed SSF-ISTBE is able to address the challenges of many emerging applications operating in dynamic and dispersive radio environments.

III. SYSTEM MODEL

We consider the cellular uplink where a mobile terminal is transmitting and a static base station is receiving. The transceiver employs STSK where the transmitter is equipped with M antennas and the receiver with N antennas. Moreover, we assume that the cardinality Q of the dispersion matrix (DM) is available to the transceiver. The transmitter architecture, shown in Fig. 1, divides the input bit stream into two bit stream subsets, one for indexing the q-th dispersion matrix and one for QAM/PSK-modulation mapping. The generated STSK codeword is stored in a buffer of size N_F symbols and the resulting block is transmitted by M cyclic-prefixed SC transmitters, employing bandlimited pulse shaping filters. The STSK codeword is generated with $log_2(Q)$ bits indexing the q-th DM, among the Q available DMs, each of size $M \times T$, where T is the duration of the STSK-codeword. The selected DM disperses the energy of the k-th input information symbol, taken from a K-ary PSK or QAM constellation. The STSKcodeword \mathbf{x}_n is then given as,

$$\mathbf{x}_n = 0 \cdot x_k A_1 + \dots + 1 \cdot x_k A_q + \dots + 0 \cdot x_k A_Q, \qquad (1)$$

where $\mathbf{x}_n \in \mathbb{C}^{M \times T}$ and only the q-th DM is activated as a result of $\log_2(Q)$ in the n-th symbol/subcarrier. It should be emphasized here that only a single DM is activated at any given time during the n-th symbol period in a block. Every column of the selected matrix is then transmitted from the M-antenna array at a baud-rate of T/T_{N_F} , where T_{N_F} is the time duration of the transmitted block.

The following parameters characterize the STSK transmission: the number of transmit antennas M, the number of receive antennas N, the cardinality Q of the set of DMs, and the codeword duration T. Specific STSK configurations are then identified as: (M,N,T,Q), where T accounts for the degree of time diversity provided that $M \geq T$.

The DM sets are generated in advance and made available to the SC-FDE system prior to transmission. The matrices are generated using the optimization rule described in [8]. A discussion of the generation process is beyond the scope of this paper.

At the receiver, the signal is first frequency down converted. After analog-to-digital (A/D) conversion and filtering, the cyclic prefix is removed from the digital STSK-aided SC signal. Then, the sample stream is serial-to-parallel converted and transformed to the frequency domain by the N_F -point Fast-Fourier Transform (FFT). We consider the channel to be quasi-static and that it remains stationary for one block period T_{N_F} [8]. Under this assumption, the received and FFT-transformed SC-STSK signal matrix \mathbf{Y} is of size $N_FN\times T$ and can be expressed as:

$$Y = HS + Z. (2)$$

H is the channel matrix of size $N_FN \times N_FM$ in the transmitted block, **Z** is the $N_F \times N$ received AWGN vector of i.i.d. components with zero-mean and σ_0^2 variance, and **S** = $[\mathbf{x}_1, \cdots, \mathbf{x}_{N_F}]$ is the block of transmitted STSK codewords of size $N_FM \times T$.

IV. PROPOSED ITERATIVE RECEIVER FOR SSF

In this section, we discuss the proposed ISTBE framework by formulating the mathematical derivation of the feedforward (FF) and the feedback (FB) filter coefficients in the presence of ideal and non-ideal HPAs.

A. The ISTBE Framework

One of the main differences between SC-FDE and OFDM is that the former does not employ the inverse-FFT (IFFT) at the transmitter side and, therefore, sub-optimal equalization in the frequency domain is the only viable solution to decode the SC-FDE signal [21]. However, the SC-FDE multi-user variant, called SC-FDMA, does employ DFT as well as IFFT in the transmitter chain for multi-user transmission. SC-FDE and OFDM exhibit the same overall computational complexity. It is worth mentioning that the performance of sub-optimal linear approaches, such as minimum mean square error (MMSE) and zero forcing (ZF), may be far from the matched filter bound (MFB) [23]. This is due to the inability of the linear equalizers to remove the existent ISI at the output of the equalization process. In order to tackle this issue, we propose a novel non-linear frequency domain turbo equalization specifically for SSF systems. Fig. 2 shows the block diagram. Prior to equalization, the signal is converted from analog to digital, followed by the CP removal. The signal Y is fed into the iterative equalization block. For the sake of clarity we drop the dimensions of the matrices. The estimated block in the frequency domain after the i-th iteration is,

$$\bar{\mathbf{S}}_i = \mathbf{F}_i \mathbf{Y} - \mathbf{B}_i \hat{\mathbf{S}}_{i-1},\tag{3}$$

where \mathbf{F}_i is an $M \times N$ matrix containing the FF coefficients for a SSF block, \mathbf{B}_i is the $M \times M$ matrix of the FB coefficients for a SSF block and $\hat{\mathbf{S}}_{i-1}$ is the estimated block of N_F symbols in the frequency domain obtained in the previous iteration. Equation (3) can also be written for n-th SSF symbol as,

$$\bar{X}_n^i = F_n^i \tilde{X}_n - B_n^i \hat{X}_n^{i-1}, \tag{4}$$

where \tilde{X}_n is the *n*-th noisy SSF symbol of received block \mathbf{Y} and \hat{X}_n^{i-1} is the *n*-th estimated SSF symbol in previous iteration. The equalized SSF symbol in *i*-th iteration is \bar{X}_n^i is obtained with the help of the coefficients and the estimated

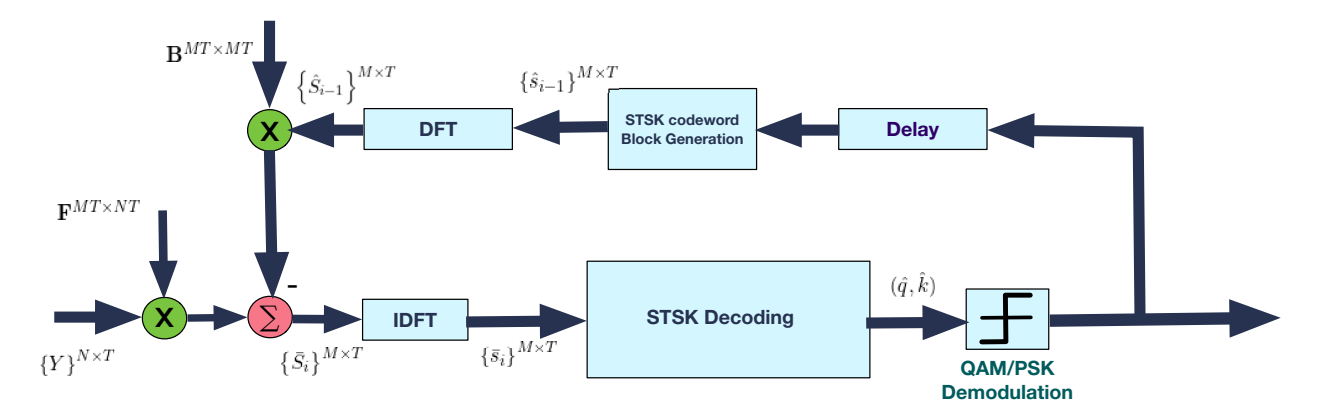


Fig. 2. The proposed ISTBE for SSF.

SSF symbol is fed back from the previous iteration, hence, the process is termed as turbo receiver. Since the interference is removed in the frequency domain, the per-symbol mean square error (MSE) at the *i*-th iteration is given as,

$$MSE^{(i)} = \frac{1}{N_F^2} \sum_{n=1}^{N_F} E\left[\left|\bar{X}_n^i - X_n\right|^2\right],$$
 (5)

Once the (5) is computed, the signal is converted into time-domain for symbol estimation. Symbol \hat{x}_n^i is the IDFT of \hat{X}_n^i . The decision block applies vectorial stacking, $vec(\cdot)$, to \hat{x}_n^i for the sake of convenience of matrix computation involved in the final decision for estimating the DM \hat{q} and symbol \hat{k} :

$$(\hat{q}, \hat{k}) = \arg\min_{q, k} \left\| \varphi_n - \kappa_n^{q, k} \right\|^2, \tag{6}$$

where,

$$\varphi_n = vec(\hat{x}_n^i) \in \mathbb{C}^{MT \times 1},$$
 (7)

$$\kappa_n^{q,k} = \mathbf{A} \chi_{q,k}^n \tag{8}$$

and A is the dispersion matrix set given as

$$\mathbf{A} = [vec(A_1), vec(A_2), \cdots, vec(A_Q)] \in \mathbb{C}^{MT \times Q}$$
 (9)

$$\chi_{q,k}^n = \left[\underbrace{0, \cdots, 0}_{q-1}, x_k^n, \underbrace{0, \cdots, 0}_{q-Q}\right]^T \in \mathbb{C}^{Q \times 1}. \tag{10}$$

Substituting (4) in (5) we get

$$MSE^{(i)} = \frac{1}{N_F^2} \sum_{n=1}^{N_F} E\left[\left| \left(F_n^i \tilde{X}_n^i - B_n^i \hat{X}_n^{i-1} \right) - X_n \right|^2 \right].$$
(11)

The MSE can be elaborated for the computation of the FB and FF coefficients; this is given in Appendix A. The persymbol MSE for each iteration depends on the computation of coefficients F_n and B_n in frequency domain. The parameters of these filters update iteratively; the FF filter is responsible for partially equalizing the residual interference and rest of it gets equalized by the FB filter. The FB filter coefficient B_n^i measures the reliability of the reconstructed interference that is subtracted from the partially equalized signal coming from the FF filter.

In order to minimize (11) such that the FB component B_n cancels out the interference from other symbols in the *i*-th iteration, we define the following constraint [23]:

$$\sum_{n=1}^{N_F} B_n^i = 0. {12}$$

Applying the Langrange multipliers method to minimize (11) yields

$$\Psi(F_n^i, B_n^i, \lambda^i) = MSE^{(i)} + \Re\left\{\lambda^i \sum_{n=1}^{N_F} B_n^i\right\}.$$
 (13)

The coefficients of (13) can be found by setting the gradient of $\Psi(F_n^i, B_n^i, \lambda^i)$ to zero, i.e.

$$\nabla_{FH}\Psi = 0
\nabla_{B^*}\Psi = 0
\nabla_{\lambda}\Psi = 0.$$
(14)

Using (41), (42) and (43), the gradients in (14) can be calculated from

$$\begin{array}{c} \bigtriangledown_{F^H} \Psi : F_n^i + F_n^i H_n^H (1 - (\rho^{i-1})^2) H_n \frac{\sigma_\chi^2}{\sigma_0^2} - H_n^H \frac{\sigma_\chi^2}{\sigma_0^2} = 0, \\ \bigtriangledown_{B^*} \Psi : F_n^i \cdot H_n - \frac{B_n^i}{\rho^{i-1}} - 1 = 0, \\ \bigtriangledown_\lambda \Psi : \sum_{n=1}^{N_F} B_n^i = 0, \end{array}$$

where σ_0^2 is the receiver noise and ρ^i is the correlation coefficient in the *i*-th iteration defined as

$$\rho^i = \frac{E\left[\hat{x}_n x_n^*\right]}{\sigma_x^2}.\tag{16}$$

Equation (15) can be further simplified for the n-th SSF symbol as,

$$F_n^i = \frac{H_n^H \frac{\sigma_X^2}{\sigma_0^2}}{1 + H_n^H (1 - (\rho^{i-1})^2) H_n \frac{\sigma_X^2}{\sigma_0^2}},$$
 (17)

$$B_n^i = \rho^{i-1} \left(F_n^i \cdot H_n - 1 \right). \tag{18}$$

For QPSK systems, the correlation coefficient ρ^i can also be obtained using the estimated SNR $\hat{\gamma}^i$ at the output of demodulation process as

$$\rho^i = 1 - 2P_b^i,\tag{19}$$

where the error probability is

$$P_b^i = Q\left(\sqrt{\hat{\gamma}^i}\right),\tag{20}$$

and $Q(u)=\frac{1}{2\pi}\int_u^\infty e^{t^2/2}dt$. Together with hard decision estimates, the correlation coefficient reduces the error propagation and thus helps with the convergence. The correlation coefficient is calculated based on the assumption that the noise at the output of equalizer is Gaussian distributed and is thus well-approximated by a Gaussian distribution. Moreover, the residual ISI can also be approximated by a Gaussian distribution from the central-limit theorem. Regarding higher order modulations, e.g. 16QAM and 64QAM, the reliability coefficient can be derived, but the derivation process is tedious due to the number of possible regions where a symbol can fall into and, hence, the final expression includes numerous terms. So an approximation is used to derive the reliability coefficient ρ as a function of the SNR at the equalizer output using the Gaussian CDF [24]:

$$\rho = \frac{1}{2} + \frac{1}{2} \operatorname{erf} \left(a \gamma_s + b \right), \tag{21}$$

where a and b are the parameters to be determined.

It is worth noting that the STSK encoder is added in the FB chain, as shown in Fig. 2, in order to reconstruct the ISI that is to be removed iteratively from the received signal. This is stated mathematically in (3). STSK-aided systems can be regarded as space-time index modulation systems where the removal of the ISI in both space and time is required for adequate performance.

B. Iterative Reduction of Nonlinear Distortion

SSPAs play a significant role in wireless communication transmitters because of their signal-amplifying characteristics. But, as the magnitude of the input signal voltage gets into the nonlinear region, this results in non-linear signal distortion [25].

The M transmitters are equipped with solid state power amplifier (SSPA) whose input-output relationship can be modeled as

$$\Xi\left[x_{n}^{m}\right] = \frac{x_{n}^{m}}{\left[1 + \left(\frac{x_{n}^{m}}{A_{o}}\right)^{2p}\right]^{\frac{1}{2p}}},\tag{22}$$

where x_n^m is the magnitude of the n-th STSK codeword symbol in the m-th transmitter chain, A_o is the output saturation level and parameter p controls the smoothness of the transition from linear to the saturation region. The phase modulation (PM) nonlinear characteristic is negligible in an SSPA. The input-output backoff (IBO-OBO) characteristics is typical for real SSPA used in wireless transmission systems and is shown in Fig. 3. The Gaussian nature of the frequency domain STSK-codeword \mathbf{S} makes the Bussgang's theorem applicable and thus, the non-linearly distorted signal block $\mathbf{S}_{(d)} = \left[\mathbf{x}_{1,(d)}, \cdots, \mathbf{x}_{N_F,(d)}\right]$ after the SSPA can be decomposed into two uncorrelated terms [26] [27]:

$$\mathbf{x}_{n,(d)} = \xi \mathbf{x}_n + \mathbf{d}_n,\tag{23}$$

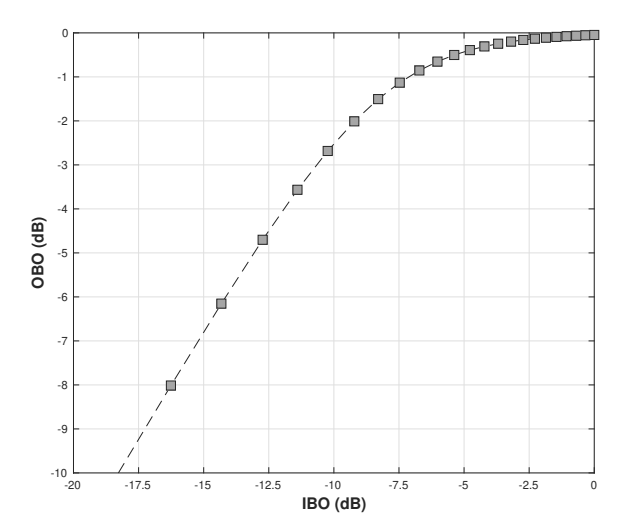


Fig. 3. IBO-OBO characteristics of the SSPA with smoothness factor $p=2,\ A_o=1$ and $A_s=2.6.$

where

$$\xi_n = \frac{E\left[\mathbf{x}_n \mathbf{x}_{n,(d)}^*\right]}{\sigma_n^2}.$$
 (24)

Parameter d is the distortion of variance σ_d^2 caused by the SSPA and is a function of the input signal envelope and the SSPA characteristics. The model that we propose can be straightforwardly extended to the Volterra series model if we need to consider memory effects in our model. However, it will increase the complexity of our simulation setup with an accuracy that will be similar to the current modeling approach. With an IBO applied to the input signal, the scaling factor is $\xi_n \to 1$ and (23) reduces to

$$\mathbf{x}_{n,(d)} = \mathbf{x}_n + \mathbf{d}_n. \tag{25}$$

The distortion term \mathbf{d}_n is confined to a single codeword symbol in the SSF-block because the CP-length of the block is larger than the multipath delay spread [27]. Moreover, \mathbf{d}_n can be combined with the AWGN term in (2) and minimized with the help of the proposed ISTBE framework. Therefore, considering the SSPA nonlinearity, (40) becomes

$$MSE_{d}^{i} = \frac{1}{N_{F}^{2}} \sum_{n=1}^{N_{F}} \left(E\left[\left| \bar{X}_{n,d}^{i} \right|^{2} \right] + \sigma_{X}^{2} - 2\Re \left\{ E\left[\bar{X}_{n,d}^{i*} X_{n} \right] \right\} \right), \tag{26}$$

where $\bar{X}_{n,d}^i$ is the estimated STSK-codeword in the presence of SSPA distortion. The derivation of the terms given in (26) is given in (27).

Moreover, we have

$$E\left[\bar{X}_{n,d}^{i*}X_{n}\right] = \sigma_{X}^{2}H_{n}^{H}F_{n}^{iH} - B_{n}^{i*}E\left[X_{n}\hat{X}_{n}^{i-1*}\right].$$
 (28)

It is worth mentioning that the distortion term D_n caused by the nonlinear distortion is uncorrelated with X_n for the n-th codeword symbol and, hence, $E[X_nD_n] \approx 0$ at any point in the ISTBE framework. Applying (27) and (28) in (26), we

derive MSE_d shown in (29). As in section IV, we apply the Langrange multipliers method to minimize the MSE in the presence of the SSPA distortion. The coefficients $F_{n,d}^i$ and $B_{n,d}^i$ can then be obtained by taking the gradient of the MSE and setting it to zero and are

$$F_{n,d}^{i} = \frac{H_n^H \frac{\sigma_X^2}{\sigma_0^2}}{1 + H_n^H (1 - (\rho^{i-1})^2) H_n \frac{\sigma_X^2 + \sigma_D^2}{\sigma_0^2}}$$
(30)

and

$$B_{n,d}^i = \rho^{i-1} \left(F_n^i \cdot H_n - \frac{\sigma_X^2}{\sigma_X^2 + \sigma_D^2} \right), \tag{31}$$

where σ_d^2 represents the distortion variance caused by the SSPA saturation and is dependent on the variance of the input signal σ_x^2 . It is worth mentioning that the MIMO-order increases the robustness against SSPA non-linearity when the number of independent data stream is fixed. As seen in Fig. 1, the energy of the single QAM/PSK-symbol disperses over M antennas (space) and T symbols (time). Hence, the variance at the output of the STSK operation is given as [28]

$$\sigma_x^2 = \left(\frac{R}{M}\right)\sigma_X^2,\tag{32}$$

where $R=\min(M,T)$ is the rank of the STSK-codeword. Parameter R denotes the number of independent streams (diversity) in the system. With increasing MIMO-order, the distortion term in (27) is $\sigma_D^2 \to 0$ and thus provides the immunity against SSPA distortions as (27) approaches (41). Such a trend is prominent in the SSF framework where the PAPR is in the 3-5 dB range.

V. SIMULATION RESULTS

Simulations have been performed with the parameters provided in Table I. An iterative pragmatic receiver [29] in the SSF framework is considered for comparison together with the SO maximum likelihood (ML) [8], SO-MMSE [10], SO-ISTBE, and the SSF-based suboptimal MMSE equalizers [21]. The pragmatic receiver is also an iterative receiver that takes the oversampled signal for equalization. More specifically, the FF and FB filter coefficients work in the oversampling domain on the SSF block as

$$\bar{\mathbf{S}}_{i}^{o} = \mathbf{F}_{i}^{o} \mathbf{Y}^{o} - \mathbf{B}_{i}^{o} \hat{\mathbf{S}}_{i-1}^{o}, \tag{33}$$

TABLE I SIMULATION PARAMETERS

Parameters	Value
Sampling Frequency	5 MSamples/sec
Bandwidth	5 MHz
Roll-off factor, α	0.20
STSK configuration	222Q & 442Q
Dispersion Matrix, Q	2, 4
Modulation Order	QPSK
Channel Model	Extended Vehicular Channel - A
Block Size	512
Iterations N_I for ISTBE	3
CP length	16

where superscript o indicates oversampling. With *a-priori* known matched pulse shape filter coefficients P, the filter coefficients F^o and B^o for the n-th subchannel can be computed as

$$F_{i,n}^{o} = \frac{\widetilde{H}_{n}^{H} P_{n}^{*} \frac{\sigma_{X}^{2}}{\sigma_{0}^{2}}}{1 + \widetilde{H}_{n}^{H} (1 - (\rho^{i-1})^{2}) \widetilde{H}_{n} \frac{\sigma_{X}^{2}}{\sigma_{0}^{2}}},$$
 (34)

$$B_{i,n}^{o} = \rho^{i-1} \left(F_{i,n}^{o} \cdot \widetilde{H}_{n} - 1 \right), \tag{35}$$

where \widetilde{H} is the oversampled version of the frequency domain channel response. After the equalization process, the signal is downsampled before demodulation.

The STSK system achieves the maximum diversity order of $N \cdot \min(M,T)$ and the matched filter bound can be computed as in [30] as

$$P_{bound} = E \left[Q \left(\frac{2E_b}{N_o} \frac{1}{M} \sum_{f=1}^{N_F} \sum_{n=1}^{N} |H_n^f|^2 \right) \right].$$
 (36)

We further assume that the channel coherence time is less than the STSK codeword duration. The roll-off factor is considered for both SO and SSF systems, which results in a spectral efficiency ρ of

$$\varrho = \frac{\log_2(Q \cdot K)}{T(1+\alpha)} \quad [bps/Hz]. \tag{37}$$

$$E\left[\left|\bar{X}_{n,d}^{i}\right|^{2}\right] = E\left[\left|F_{n}^{i}(\tilde{X}_{n}^{i} + \tilde{D}_{n}^{i}) - B_{n}^{i}(\hat{X}_{n}^{i-1} + \hat{D}_{n}^{i-1})\right|^{2}\right]$$

$$= H_{n}^{H}H_{n}F_{n}^{i}F_{n}^{iH}\left(\sigma_{X}^{2} + \sigma_{D}^{2}\right) + \left|B_{n}^{i}\right|^{2}\sigma_{\hat{X}}^{2} + \left|B_{n}^{i}\right|^{2}\sigma_{\hat{D}}^{2} - 2\Re\left\{B_{n}^{i*}F_{n}^{i}H_{n}\left[E\left[X_{n}^{i}\hat{X}_{n}^{i-1*}\right] + E\left[D_{n}^{i}\hat{D}_{n}^{i-1*}\right]\right]\right\}.$$
(27)

$$MSE_{d}^{i} = \frac{1}{N_{F}^{2}} \sum_{n=1}^{N_{F}} \left\{ H_{n} H_{n}^{H} F_{n}^{i} F_{n}^{iH} \left(\sigma_{X_{n}}^{2} + \sigma_{D_{n}}^{2} \right) + \left| B_{n}^{i} \right|^{2} \sigma_{X_{n}}^{2} + \left| B_{n}^{i} \right|^{2} \sigma_{D_{n}}^{2} - 2\Re \left\{ B_{n}^{i*} F_{n}^{i} H_{n} \left(E \left[X_{n}^{i} \hat{X}_{n}^{i-1*} \right] + E \left[D_{n}^{i} \hat{D}_{n}^{i-1*} \right] \right) \right\} + \sigma_{X_{n}}^{2} - 2\Re \left\{ \sigma_{X_{n}}^{2} H_{n}^{H} F_{n}^{iH} - B_{n}^{i*} E \left[X_{n} \hat{X}_{n}^{i-1*} \right] \right\} \right\}.$$

$$(29)$$

A. Convergence Analysis of the SSF-ISTBE

Because of its iterative nature, it is important to analyze the behavior of the ISTBE as a function of the number of iterations N_I . Indeed, N_I drives the computational complexity of the proposed framework and is further discussed in Section V-C. It is therefore important to converge to a stable performance within a few iterations so that the computational complexity remains low. In this regard, Fig. 4 shows the convergence performance of the ISTBE for the considered STSK configurations for a fixed E_b/N_o of 8 dB. With $N_I=3$ the SSF-ISTBE systems converges, thus confirming its suitability. The iterative pragmatic receiver converges to a higher BER because of the increased in-phase/quadrature interference (IQI) and ISI. This is further discussed in the next subsection. Note that at $N_I = 1$, the ISTBE is equivalent to the MMSE receiver as ρ^i is 0 in (19) for the first iteration. However, as the iteration process takes its course, the ISTBE is able to remove the inherent interference and nonlinear distortion, where applicable, resulting in a significant increase in performance over the MMSE receivers.

B. Link Performance Analysis

First we consider the (2,2,2,2) configuration. The results are shown in Fig. 5. This configuration offers a spectral efficiency of $\varrho = 1.25$ bps/Hz. The proposed framework, SSF with ISTBE, has proven to be the suitable candidate for systems with relaxed data rate requirements. The SSF-ISTBE is able to achieve gains as high as 4 dB over the SSF-MMSE, 2 dB over the SSF-based pragmatic receiver and 3 dB over the SO-ML for $E_b/N_o \geq 10$ dB. The SSF-based pragmatic receiver equalizes the oversampled received signal while computing the feedforward and feeback filter coefficient. As a result, the filtering process becomes complex and yields a complex overall impulse response at the equalizer's output. This gives rise to significant IQI and ISI, which bound the performance in the high SNR regime. On the other hand, the ISTBE effectively removes the inherent ISI that severely bounds the performance of the SSF when sub-optimal linear

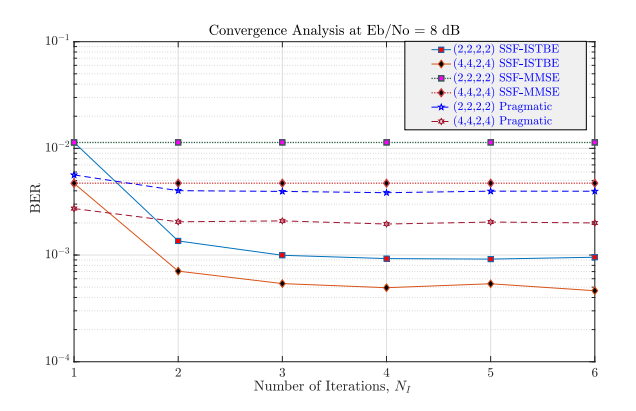


Fig. 4. Convergence of the proposed SSF-ISTBE and state-of-the-art receivers for the considered STSK configurations at $E_b/N_o=8$ dB. The convergence line indicates iteration number N_I at which the BER remains the same for subsequent iterations.

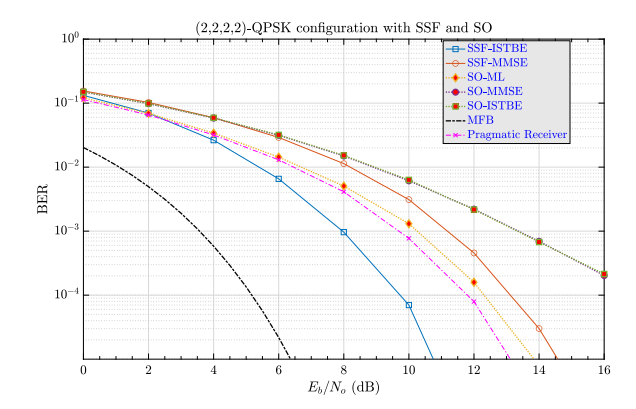


Fig. 5. Performance of the ISTBE and state-of-the-art receivers for SSF and SO in the extended vehicular channel-A with ideal RF front ends. The spectral efficiency is $\varrho=1.25$ and the roll-off factor $\alpha=0.2$.

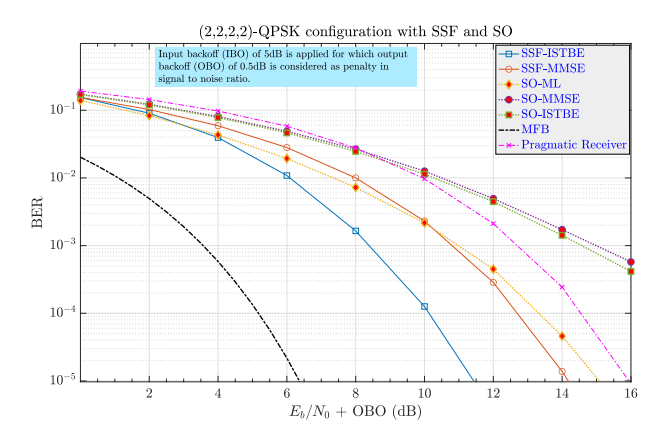


Fig. 6. Performance of the ISTBE and state-of-the-art receivers for SSF and SO in the extended vehicular channel-A. A non-linear SSPA is considered with p=2. The spectral efficiency is $\varrho=1.25$ and the roll-off factor is $\alpha=0.2$.

techniques are employed. It is important to note that the SO-ISTBE framework is reduced to SO-MMSE in terms of performance and computation because of the orthogonality among subcarriers and the negligible inherent ISI.

In order to evaluate the performance of the ISTBE scheme with a higher single-user spectral efficiency of $\rho = 1.667$ bps/Hz, we increase the dispersion matrix cardinality Q to 4. Without loss of generality, we choose (4,4,2,4)-QPSK as the STSK configuration. In this configuration the eigenvalues of the DM set are (0.0000, 0.0000, 0.9422, 2.2876). Practically speaking, the DM set has a rank of 2 because the remaining two values are negligible. Hence, the transmit diversity order will remain 2 as in (2,2,2,2). So the performance will be comparable to (2,2,2,2) with a higher ϱ , as seen in Fig. 7. We observe that the proposed SSF-ISTBE outperforms all the considered receiver designs for both SO and SSF by exploiting diversity, where a gain margin of 4 dB is observed over SSFpragmatic and SSF-MMSE in rich scattering environments of typical frequency selective channels. The SSF-based oversampled pragmatic receiver cannot exploit the diversity because

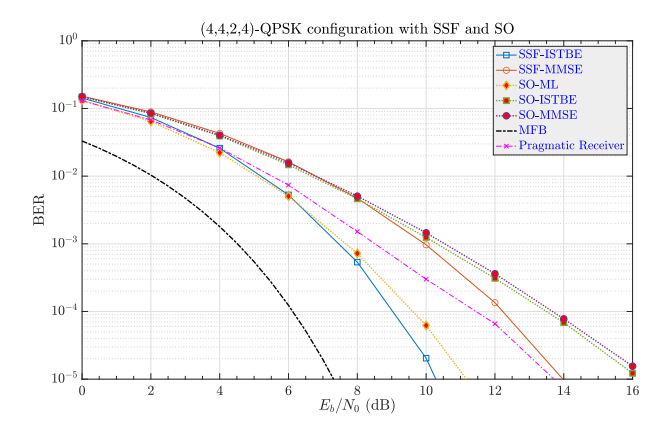


Fig. 7. Performance of the ISTBE and state-of-the-art receivers for SSF and SO in the extended vehicular channel-A with ideal RF front ends. The spectral efficiency is $\rho = 1.667$ and the roll-off factor $\alpha = 0.2$.

TABLE II SSPA input backoff values.

	(2,2,2,2)-QPSK	(4,4,2,4)-QPSK
SSF	IBO = 5 dB	IBO = 0 dB
SO	IBO = 5 dB	IBO = 5 dB

of the highly correlated subchannels. Its performance thus deteriorates in the high SNR regime, as shown in Fig. 7. In the next set of results, we present the comparison between SSF and SO in the presence of a non-linear SSPA in the transmitter. The backoff values are reported in Table II. The backoff values are computed from average values of waveforms. Notice that the IBO values are not high because considering QPSK as opposed to higher order quadrature-amplitude modulation schemes. We can see from Fig. 6 that the performance of the SSF with the proposed receiver outperforms the rest of the considered systems considering practical RF hardware impairments and mitigation techniques. The underlying STSKconfiguration allows R = 2 and, hence, even systems like SSF (exhibiting low PAPR) require 5 dB IBO. With the help of Fig. 3, the corresponding OBO of 0.5 dB as the SNR penalty is applied in all the cases. The non-linear SSPA severely impacts the performance of the pragmatic receiver resulting in 5 dB loss with respect to the proposed SSF-ISTBE receiver in the high SNR regime. The SSPA adversely effects SO systems due to clipping of envelope fluctuations which makes the transmitter less power efficient. Therefore, the SNR decreases and the BER increases. This trend is clearly visible in the high SNR regime where the proposed SSF outperforms the SO-ML with a margin of 4 dB.

Increasing the MIMO-order allows to disperse the input QPSK-modulated symbol energy over a large number of transmitter chains. Because of (32), the input signal energy in each RF chain is reduced and, hence, the SSPA operates in the linear region. This is an advantage of SSF systems, where the SSPA saturation does not impact the performance. However, SO systems are still required to operate with IBO of 5 dB in this use case. As shown in Fig. 8, the proposed SSF-ISTBE enables performance improvements over SO-ML

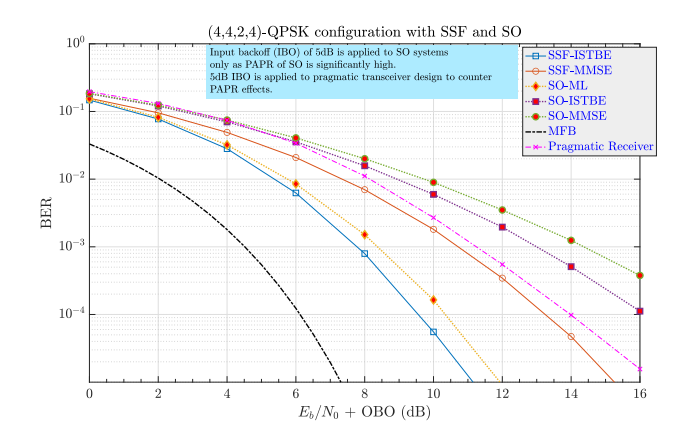


Fig. 8. Performance of the ISTBE and state-of-the-art receivers for SSF and SO in the extended vehicular channel-A. A non-linear SSPA is considered with p=2. The spectral efficiency is $\varrho=1.667$ and the roll-off factor $\alpha=0.2$

with a margin of around 2 dB. In addition, the SSF-ISTBE does not employ an IBO and, hence, is more power efficient compared to the SO system. The situation is much worse for the pragmatic receiver because of the highly correlated subchannels that do not yield a diversity gain and the nonlinear effects of the SSPA with the necessary IBO.

With reduced diversity order $T \leq M$, the SSF-MMSE receiver does not fully exploit the diversity and the spectral efficiency decreases (Fig. 8). A similar trend can be seen for SO-MMSE where the BER decays slowly with SNR in the presence of non-linear SSPAs that are found in practical systems.

C. Computational Complexity

The computational complexity analysis here provides insights into the computations involved in demodulating the received signal. We investigate the computational complexity of the proposed ISTBE against the ones proposed in recent literature: SO-ML [8], SSF-MMSE [21], SSF-pragmatic, and SSF-ML. The SSF-ISTBE framework requires channel state information (CSI) at the receiver for coherent detection of the source information in every iteration to update the FF coefficients. Therefore, it poses a slightly higher, yet affordable computational complexity with respect to the system presented in [21]. The computational complexities of the proposed and the state-of-the-art schemes are measured in terms of the number of real-valued multiplications and are captured in Table III.

The complexity associated with the computation of the frequency domain FF coefficients F of the ISTBE is

$$comp \left[\left[1 + H_n^H (1 - (\rho^{i-1})^2) H_n \frac{\sigma_X^2}{\sigma_0^2} \right]^{-1} H_n^H \frac{\sigma_X^2}{\sigma_0^2} \right]$$

$$= 4MN (M+1),$$
(38)

where H_n is the channel response for the n-th codeword symbol, ρ is the reliability coefficient, and $\frac{\sigma_X^2}{\sigma_0^2}$ is the channel SNR. The complexity involved in the estimation of the

TABLE III
COMPUTATIONAL COMPLEXITIES OF THE PROPOSED AND THE CORRESPONDING STATE-OF-THE-ART DETECTION SCHEMES

Receiver	Computational complexity per bit
SSF-MMSE	$4M^2N + 8MN + 4MTQ + 2QK' + Q + 2K$
SO-ML	4MNTQ + 4NTQL + 2NTQL
SSF-ML	$(Q\cdot K)^{N_F}$
SSF-ISTBE	$N_I (4MN(M+2) + 4MTQ + Q + 2QK' + 2K + 2N_F \log_2(N_F) + N_F MT + 4MNT)$
SSF-pragmatic	$N_{I}\left(4OvMN(M+2)+4MTQ+Q+2QK'+2K+2N_{F}\log_{2}(N_{F})+N_{F}MT+4OvMNT\right)$

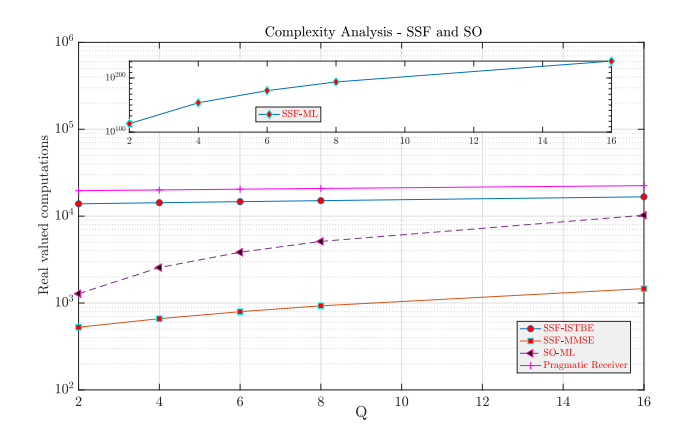


Fig. 9. Computational complexity of the SO and SSF receivers with M = 4, N = 4, $N_F=128,\, {\rm T}=4$ and $N_I=3.$

DM index \hat{q} and the symbol \hat{k} as given in (6)-(10) is 4MN + 4MTQ + Q + 2QK' + 2K. The two IFFT/FFT operations and the STSK-encoding in the feedback loop require $2N_F \log_2(N_F)$ and N_FMT real multiplications, respectively. Therefore, the overall complexity in terms of real-valued multiplications per iteration is given as

complexity =
$$4MN(M+2) + 4MTQ + Q + 2QK'$$

+ $2K + 2N_F \log_2(N_F) + N_F MT + 4MNT$
(39)

Fig. 9 illustrates this. It is worth mentioning that the complexity of the ISTBE is almost constant with respect to the DM cardinality in logrithmic scale. The overall complexity order is driven by the block length N_F . The order of magnitude increase when compared to practical legacy equalizers is reasonable for today's transceivers.

VI. CONCLUSIONS & FUTURE WORK

In this work we propose an SSF framework for the uplink of mobile wireless systems, enabling diversity gains over state-of-the-art iterative SSF receivers and SO solutions with optimal and sub-optimal receivers in dispersive channels. The performance gain of the SSF-ISTBE is shown to be significant also when non-linear distortions are present in the system along with multipath propagation. Albeit the reduced computational complexity of linear systems, specifically SSF-MMSE and

SO-MMSE, the performances of these systems are quite far from the matched filter bound. The proposed framework is able to achieve near-optimum performance by minimizing the inherent ISI with an affordable computational complexity increase over linear equalizers.

In future work, we will develop a multiuser framework for the STSK-aided SC-FDMA with the proposed receiver design. Another important aspect to be considered is the practical implementation of such a receiver design using softwaredefined radios (SDRs). In this regard, software prototyping can be performed with GNU Radio which allows to experimentally assess the performance in RF field experiments. Example applications of the proposed framework can be found in the context of the AERPAW project [31] aimed at implementing and testing emerging and new broadband technology and applications to accelerate advances of unmanned aerial systems using a practical testbed in a large-scale production environment. The spectral efficiency, energy efficiency, and adequate BER performance in dispersive environments makes the SSF-ISTBE a viable solution for emerging wireless contexts and suitable for development and testing using SDRs and the AERPAW testbed. In such a framework, the impact of terminal mobility on the algorithmic performance can be assessed as a function of practical time varying channel characterizations, channel state information outages, and Doppler frequencies, among others.

Appendix A

MATHEMATICAL MANIPULATION OF THE MEAN SQUARE ERROR IN THE PROPOSED RECEIVER

The mathematical formulation of the MSE is important to derive the feedback **B** and feedforward **F** coefficients for the ISTBE receiver in the SSF-framework.

Considering ideal channel estimation \mathbf{H} available at the receiver, for the n-th symbol using (5) we get

$$MSE^{i} = \frac{1}{N_{F}^{2}} \sum_{n=1}^{N_{F}} \left(E\left[\left| \bar{X}_{n}^{i} \right|^{2} \right] + \sigma_{X}^{2} - 2\Re \left\{ E\left[\bar{X}_{n}^{i*} X_{n} \right] \right\} \right). \tag{40}$$

With the help of (4) and (40), we obtain the statistical terms

$$E\left[\left|\bar{X}_{n}^{i}\right|^{2}\right] = E\left[\left|F_{n}^{i}\tilde{X}_{n}^{i} - B_{n}^{i}\hat{X}_{n}^{i-1}\right|^{2}\right]$$

$$= F_{n}^{i}E\left[\tilde{X}_{n}^{i}\tilde{X}_{n}^{i*}\right]F_{n}^{iH} + \left|B_{n}^{i}\right|^{2}\sigma_{\hat{X}}^{2} -$$

$$2\Re\left\{B_{n}^{i*}F_{n}^{i}H_{n}E\left[\tilde{X}_{n}^{i}\hat{X}_{n}^{i-1*}\right]\right\},$$
(41)

$$E\left[\tilde{X}_{n}^{i}\tilde{X}_{n}^{i*}\right] = \sigma_{\tilde{X}}^{2}H_{n}H_{n}^{H} + \sigma_{0}^{2}\mathbb{I}_{N},\tag{42}$$

and

$$E\left[\bar{X}_{n}^{i*}X_{n}\right] = \sigma_{X}^{2}H_{n}^{H}\left(F_{n}^{iH}\right) - B_{n}^{i*}E\left[X_{n}\hat{X}_{n}^{i-1*}\right]. \tag{43}$$

ACKNOWLEDGEMENT

The work of V. Marojevic is supported in part by the National Science Foundation under grant number CNS-1564148.

REFERENCES

- [1] M. Alsenwi, N. H. Tran, M. Bennis, S. R. Pandey, A. K. Bairagi, and C. S. Hong, "Intelligent resource slicing for eMBB and URLLC coexistence in 5G and beyond: A deep reinforcement learning based approach," *IEEE Transactions on Wireless Communications*, 2021.
- [2] F. Tariq, M. R. Khandaker, K.-K. Wong, M. A. Imran, M. Bennis, and M. Debbah, "A speculative study on 6G," *IEEE Wireless Communications*, vol. 27, no. 4, pp. 118–125, 2020.
- [3] Z. Wang, X. Ma, and G. B. Giannakis, "OFDM or single-carrier block transmissions?" *IEEE transactions on communications*, vol. 52, no. 3, pp. 380–394, 2004.
- [4] F. Silva, R. Dinis, and P. Montezuma, "Frequency-domain receiver design for transmission through multipath channels with strong doppler effects," Wireless Personal Communications, vol. 83, no. 2, pp. 1213– 1228, 2015.
- [5] R. Y. Mesleh, H. Haas, S. Sinanovic, C. W. Ahn, and S. Yun, "Spatial modulation," *IEEE Transactions on vehicular technology*, vol. 57, no. 4, pp. 2228–2241, 2008.
- [6] P. W. Wolniansky, G. J. Foschini, G. D. Golden, and R. A. Valenzuela, "V-BLAST: An architecture for realizing very high data rates over the rich-scattering wireless channel," in 1998 URSI international symposium on signals, systems, and electronics. Conference proceedings (Cat. No. 98EX167). IEEE, 1998, pp. 295–300.
- [7] S. M. Alamouti, "A simple transmit diversity technique for wireless communications," *IEEE Journal on selected areas in communications*, vol. 16, no. 8, pp. 1451–1458, 1998.
- [8] S. Sugiura, S. Chen, and L. Hanzo, "Coherent and Differential Space-Time Shift Keying: A Dispersion Matrix Approach," *IEEE Transactions* on Communications, vol. 58, no. 11, pp. 3219–3230, 2010.
- [9] C. Sacchi, T. F. Rahman, I. A. Hemadeh, and M. El-Hajjar, "Millimeter-wave transmission for small-cell backhaul in dense urban environment: A solution based on MIMO-OFDM and space-time shift keying (STSK)," *IEEE Access*, vol. 5, pp. 4000–4017, 2017.
- [10] M. I. Kadir, S. Sugiura, J. Zhang, S. Chen, and L. Hanzo, "OFDMA/SC-FDMA aided space-time shift keying for dispersive multiuser scenarios," *IEEE transactions on vehicular technology*, vol. 62, no. 1, pp. 408–414, 2012.
- [11] T. F. Rahman and C. Sacchi, "Space-Time Shift Keying and Constant-Envelope OFDM: A New Solution for Future Mm-Wave MIMO Multicarrier Systems," in 2018 European Conference on Networks and Communications (EuCNC). IEEE, 2018, pp. 103–9.
- [12] T. F. Rahman, C. Sacchi, S. Morosi, A. Mazzinghi, and N. Bartolomei, "Constant-envelope multicarrier waveforms for millimeter wave 5G applications," *IEEE Transactions on Vehicular Technology*, vol. 67, no. 10, pp. 9406–9420, 2018.
- [13] S. Buzzi, C. D'Andrea, T. Foggi, A. Ugolini, and G. Colavolpe, "Single-carrier modulation versus OFDM for millimeter-wave wireless MIMO," *IEEE Transactions on Communications*, vol. 66, no. 3, pp. 1335–1348, 2017.
- [14] N. Benvenuto and S. Tomasin, "Iterative design and detection of a DFE in the frequency domain," *IEEE Transactions on Communications*, vol. 53, no. 11, pp. 1867–1875, 2005.
 [15] D. Fernandes, F. Cercas, and R. Dinis, "Analytical Performance Eval-
- [15] D. Fernandes, F. Cercas, and R. Dinis, "Analytical Performance Evaluation of Massive MIMO Techniques for SC-FDE Modulations," *Electronics*, vol. 9, no. 3, p. 533, 2020.

- [16] L. Xiao, Y. Xiao, Y. Zhao, P. Yang, M. Di Renzo, S. Li, and W. Xiang, "Time-Domain Turbo Equalization for Single-Carrier Generalized Spatial Modulation," *IEEE Transactions on Wireless Communications*, vol. 16, no. 9, pp. 5702–5716, 2017.
- [17] Y. Zhao, P. Yang, Y. Xiao, L. Xiao, B. Dong, and W. Xiang, "An improved frequency domain turbo equalizer for single-carrier spatial modulation systems," *IEEE Transactions on Vehicular Technology*, vol. 66, no. 8, pp. 7568–7572, 2017.
- [18] L. He, J. Wang, and J. Song, "Information-aided iterative equalization: A novel approach for single-carrier spatial modulation in dispersive channels," *IEEE Transactions on Vehicular Technology*, vol. 66, no. 5, pp. 4448–4452, 2016.
- [19] Y. Zhao, Y. Xiao, P. Yang, B. Dong, R. Shi, and K. Deng, "Generalized approximate message passing aided frequency domain turbo equalizer for single-carrier spatial modulation," *IEEE Transactions on Vehicular Technology*, vol. 67, no. 4, pp. 3630–3634, 2017.
- [20] S. Lin, B. Zheng, F. Chen, F. Ji, and H. Yu, "Soft Demodulators Based on Deterministic SMC for Single-Carrier GSM in Broadband Channels," *IEEE Journal on Selected Areas in Communications*, vol. 37, no. 9, pp. 1973–1985, 2019.
- [21] T. F. Rahman, A. Habib, C. Sacchi, and M. El-Hajjar, "Mm-wave STSK-aided single carrier block transmission for broadband networking," in 2017 IEEE Symposium on Computers and Communications (ISCC). IEEE, 2017, pp. 507–514.
- [22] J. Choi, "Single-carrier index modulation for IoT uplink," *IEEE Journal of Selected Topics in Signal Processing*, vol. 13, no. 6, pp. 1237–1248, 2019
- [23] C. Zhang, Z. Wang, C. Pan, S. Chen, and L. Hanzo, "Low-complexity iterative frequency domain decision feedback equalization," *IEEE Trans*actions on Vehicular Technology, vol. 60, no. 3, pp. 1295–1301, 2011.
- [24] G. Huang, A. Nix, and S. Armour, "Feedback reliability calculation for an iterative block decision feedback equalizer," in 2009 IEEE 70th Vehicular Technology Conference Fall. IEEE, 2009, pp. 1–5.
- [25] M. Shabany and P. G. Gulak, "Efficient compensation of the nonlinearity of solid-state power amplifiers using adaptive sequential Monte Carlo methods," *IEEE Transactions on Circuits and Systems I: Regular Papers*, vol. 55, no. 10, pp. 3270–3283, 2008.
- [26] J. J. Bussgang, "Crosscorrelation functions of amplitude-distorted Gaussian signals," Research Laboratory of Electronics, Massachusetts Institute of Technology, 1952.
- [27] J. Tellado, L. M. Hoo, and J. M. Cioffi, "Maximum-likelihood detection of nonlinearly distorted multicarrier symbols by iterative decoding," *IEEE transactions on communications*, vol. 51, no. 2, pp. 218–228, 2003.
- [28] J. Guerreiro, R. Dinis, and P. Montezuma, "On the assessment of nonlinear distortion effects in MIMO-OFDM systems," in 2016 IEEE 83rd Vehicular Technology Conference (VTC Spring). IEEE, 2016, pp. 1–5.
- [29] P. Bento, A. Pereira, R. Dinis, M. Gomes, and V. Silva, "Low-Complexity Equalisers for Offset Constellations in Massive MIMO Schemes," *IEEE Access*, vol. 7, pp. 94 373–94 390, 2019.
- [30] F. Silva, R. Dinis, N. Souto, and P. Montezuma, "Approaching the matched filter bound with block transmission techniques," *Transactions* on *Emerging Telecommunications Technologies*, vol. 23, no. 1, pp. 76– 85, 2012.
- [31] V. Marojevic, I. Guvenc, R. Dutta, M. L. Sichitiu, and B. A. Floyd, "Advanced Wireless for Unmanned Aerial Systems: 5G Standardization, Research Challenges, and AERPAW Architecture," *IEEE Vehicular Technology Magazine*, vol. 15, no. 2, pp. 22–30, 2020.



Talha Faizur Rahman received the Masters degree and Ph.D. degree in Information and Communication Technology from the University of Trento, Italy, in 2012 and 2015, respectively. From 2007 to 2018, he worked in Centre for Advanced Studies in Telecommunications (CAST) at

COMSATS University Islamabad in different capacities. Since 2018, he has attained multiple academic and industrial positions in Italy and Poland. Starting from March 2021, he has been working as postdoctoral researcher at Mississippi State University on different NSF-funded projects, namely

AERPAW and OAIC. His research interests include, wireless communications, Internet of Things, Software Defined Radios and GNU-radio.



Vuk Marojevic (SM'18) is an associate professor in ECE at Mississippi State University, Starkville, MS, USA. He is a principal investigator of the NSF projects AERPAW and Open Artificial Intelligence Cellular (OAIC). His research interests include mobile communications and wireless security with application to mission-critical networks and unmanned aircraft systems.

He is an associate editor of the IEEE Transactions on Vehicular Technology and the IEEE Vehicular Technology Magazine.



Claudio Sacchi (M'01–SM'07) received the Laurea degree in electronic engineering and the Ph.D. degree in space science and engineering from the University of Genoa, Italy, in 1992 and 2003, respectively. From 1996 to 2002, he was a Research Cooperator with the Department of Biophysical and Electronic Engineering (DIBE), University of Genoa, and with the National Italian Consortium in

Telecommunications (CNIT), managing project activities in the field of multimedia surveillance systems and satellite communications. Since August 2002, he has joined the Department of Information Engineering and Computer Science (DISI), University of Trento, Italy, covering the role of an Assistant Professor. He is also with the Research Unit at the University of Trento, CNIT. He upgraded to the position of an Associate Professor in December 2020. He has authored and coauthored more than 110 papers published in international journals and conferences. His research interests are mainly focused on wideband mobile and satellite transmission systems based on space, time and frequency diversity, MIMO systems, array processing; multi-rate and multi-access wireless communications; EHF broadband aerospace communications; software radio and cognitive radio; and radio communications for emergency recovery applications. In 2011, he was a Guest Editor of the special issue of PROCEEDINGS OF THE IEEE: Aerospace Communications: History, Trends and Future and the featuredtopic special issue of IEEE Communications Magazine: Toward the Space 2.0 Era in 2015. Since 2019, he has been coordinating and chairing the IEEE AESS technical panel: "Glue Technologies for Space Systems" that was awarded by AESS as "Outstanding Panel of the year 2020." He is a member of the IEEE ComSoc, IEEE BTS, IEEE VT, and IEEE AESS Society.